Supporting information

Higher and lower supramolecular order for the design of self-assembled heterochiral tripeptide hydrogel biomaterials

S. Marchesan*[a,b] K. E. Styan[b], C. D. Easton[b], L. Waddington[b], and A. V. Vargiu[c].

[a] University of Trieste, Chemical and Pharmaceutical Sc. Dep., Center of Excellence for Nanostructured Materials (CENMAT), Via L. Giorgieri 1, 34127 Trieste, Italy.
* corresponding author. email: smarchesan@units.it
[b] CSIRO Manufacturing Flagship, Clayton, VIC 3168, Australia
[c] University of Cagliari, Department of Physics, Cittadella Universitaria S. P. Monserrato-Sestu Km. 0.700, 09042 Monserrato (CA), Italy

Table of Contents **Page**

1. Rheometric data for the four gelling tripeptides.

vFF

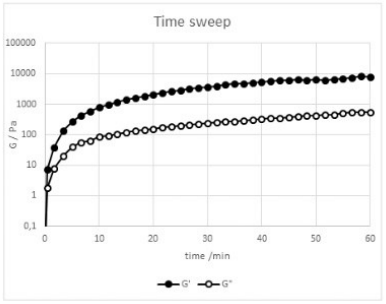

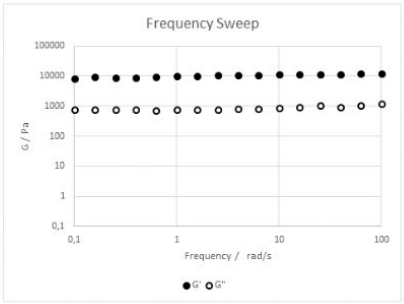

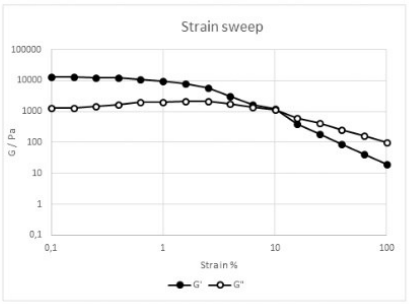

Vff

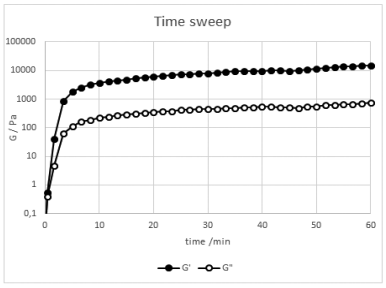

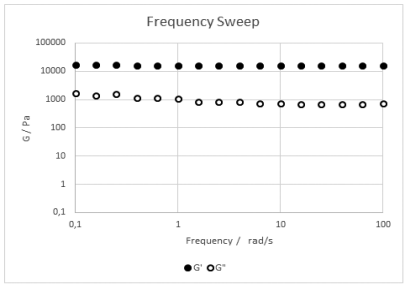

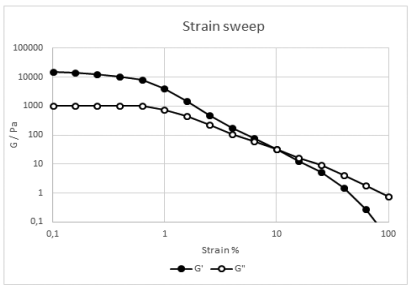

VfF

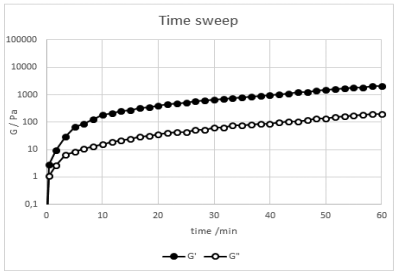

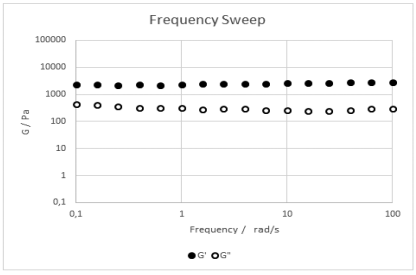

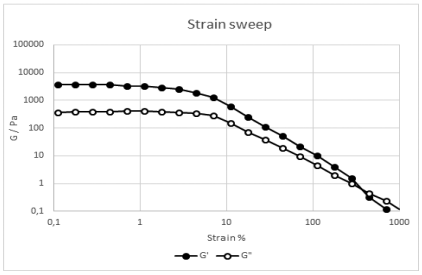

vFf

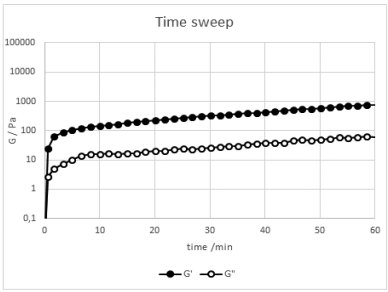

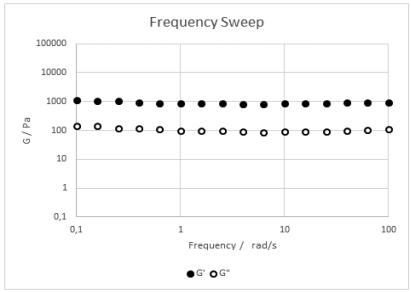

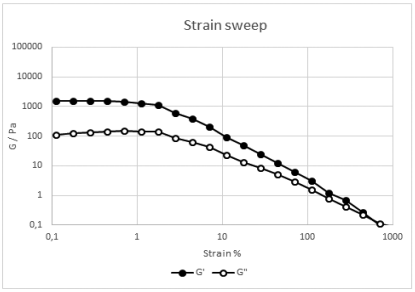

2. DSC data for the four gels

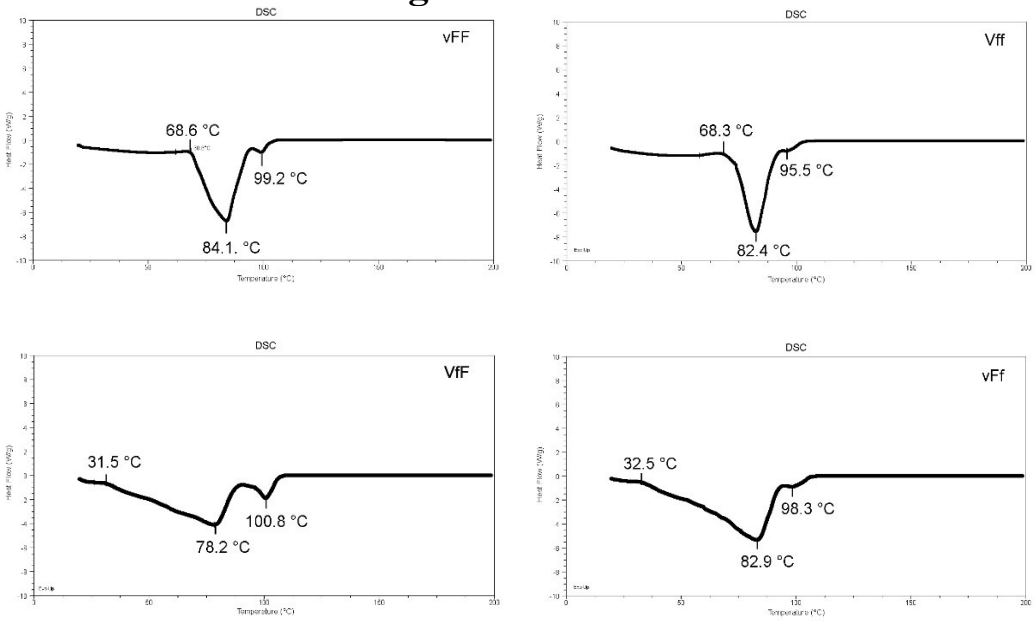

3. FT-IR spectra of non-gelling tripeptides

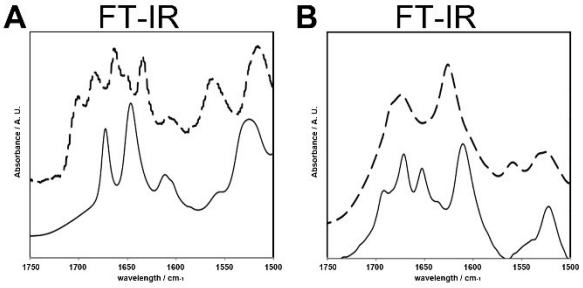

FT-IR spectra of the four non-gelling tripeptides. A. Enantiomers vfF (dashed line) and VFf (black line). B. Enantiomers vff (dashed line) and VFF (black line).

4. CD spectra of non-gelling tripeptides

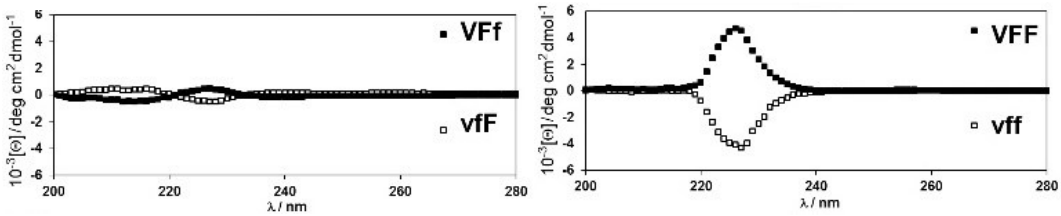

CD spectra of heterochiral non-gelling tripeptides (left) reveal a weak signal for beta-sheets and aromatic stacking. CD spectra of the homochiral tripeptides (right) show only a marked signal for aromatic stacking.

5. Thioflavin-T imaging of the non-gelling tripeptides

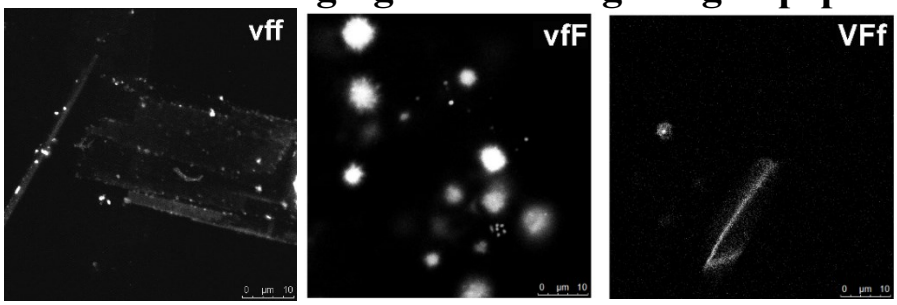

Thioflavin T-stained fluorescence microscopy images of non-gelling tripeptides. NOTE: Brightness was notably increased in these images to visualize the occasional, dim structures. Nevertheless, no structure was at all visible for VFF (not shown). Extremely dim plate crystals with spherical nucleating regions were occasionally seen for vff (left) similarly to what we reported for the homochiral tripeptide Leu-Phe-Phe (S. Marchesan et al. Nanoscale 2012). The other heterochiral tripeptides vfF and VFf displayed only occasional spherical nucleating regions that would coalesce into larger ones, and a few elongated structures (centre and right).

6. Cryo-TEM images of non-gelling tripeptides

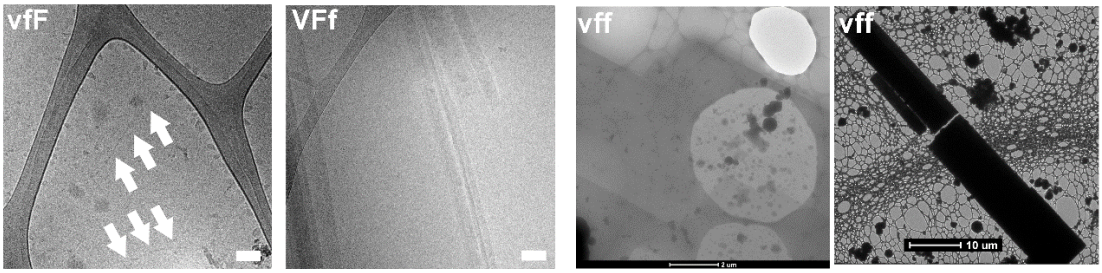

Cryo-TEM revealed structures that were consistent with Thioflavin-T stained imaging. Heterochiral tripeptides vfF and VFf formed isolated, occasional structures consisting of nanotapes (white arrows). Homochiral vff formed only occasional plate crystals most of which were too large to image well by cryoTEM, or even to embed in ice (far right).

7. Cytotoxicity assay for the gelling tripeptides in solution

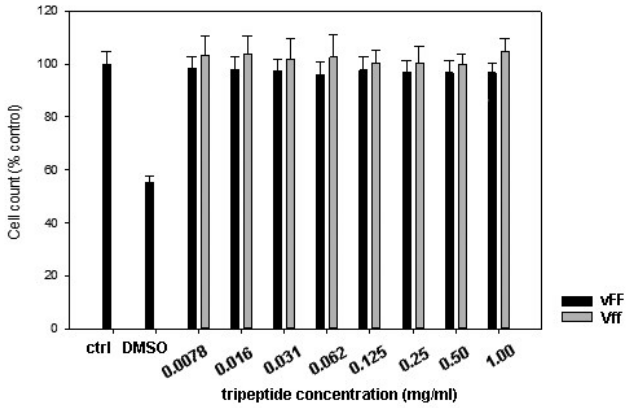

Cytotoxicity assay according to ISO 10993 shows that the gelling tripeptides in solution are non-toxic to fibroblast cells. Average values ± SD, within a single replicate experiment, are shown.

8. Spectroscopic data for VfF

^{1}H-NMR (400 MHz, DMSO-d_6, TMS): δ 8.67 (d, J = 8 Hz, 1H, NH), 8.58 (d, J = 8 Hz, 1H, NH), 7.29-7.11 (m, 10H, Ar), 4.78 (m, 1H, αCH), 4.51 (m, 1H, αCH), 3.53 (m, 1H, αCH), 3.12 (dd, J = 4 and 12 Hz, 1H, βCH$_2$), 2.84 (dd, J = 8 and 12 Hz, 1H, βCH$_2$), 2.66 (dd, J = 4 and 12 Hz, 1H, βCH$_2$), 2.39 (dd, J = 8 and 12 Hz, 1H, βCH$_2$), 1.80 (m, 1H, βCH) 0.65 (d, 3H, γCH$_3$), 0.40 (d, 3H, γCH$_3$). ^{13}C-NMR (100MHz, DMSO-d_6, TMS): δ (ppm) 173.5, 171.1, 168.1 (3 x CO); 138.0, 137.8, 129.8, 129.6, 128.5, 128.4, 126.9, 126.7 (Ar); 57.7, 54.1, 53.9, (3 x αC); 38.8, 37.8 (2 x βCH$_2$); 30.0 (βCH); 18.7, 16.8 (2 x γCH$_3$). MS (ESI): m/z 412.1 $(M+H)^+$, $C_{23}H_{29}N_3O_4$ requires 412.2.

^{1}H-NMR (400 MHz, DMSO-d_6, TMS)

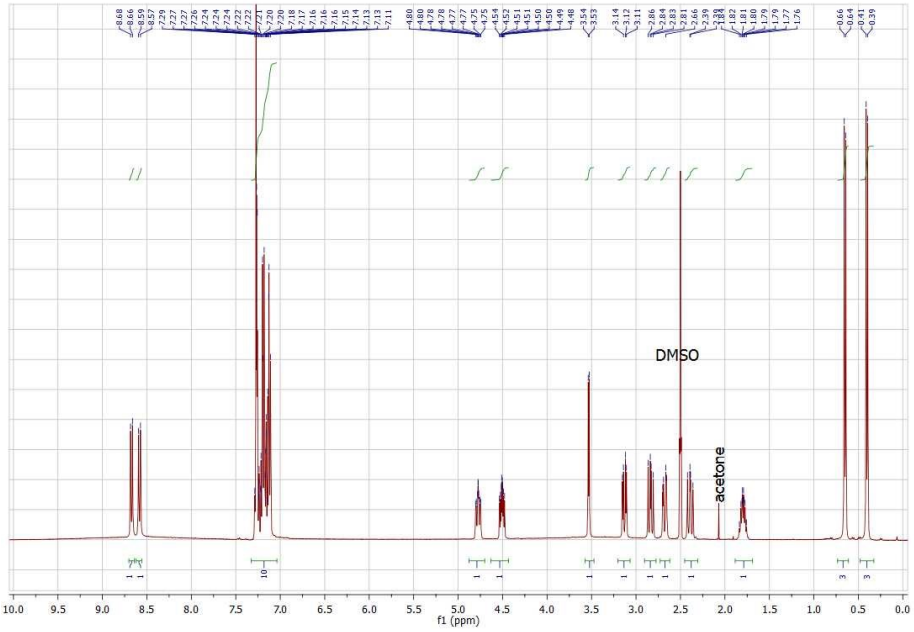

^{13}C-NMR (100MHz, DMSO-d_6, TMS)

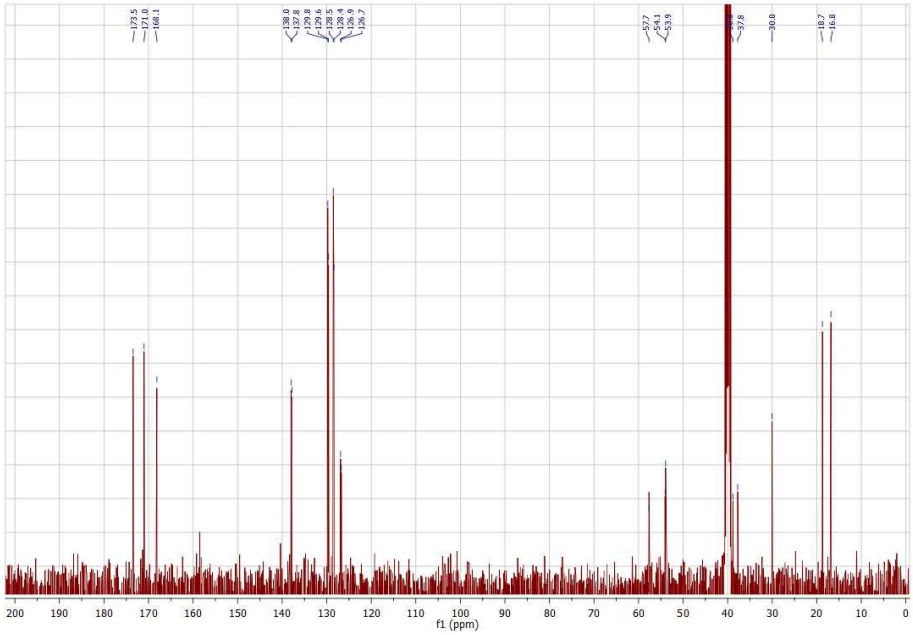

HPLC

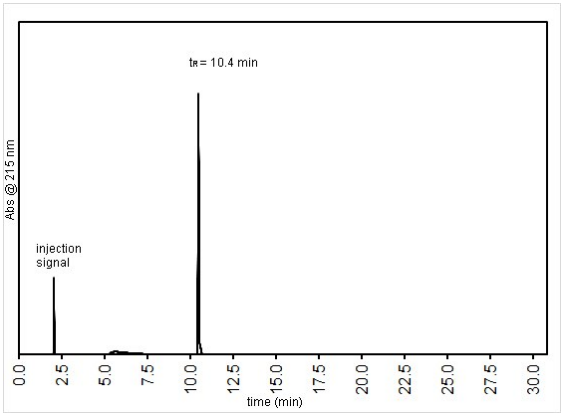

ESI-MS

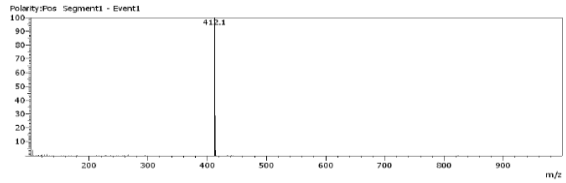

9. Spectroscopic data for VFf

^{1}H-NMR (400 MHz, DMSO-*d*$_6$, TMS): δ (ppm) 8.46 (d, *J* = 8 Hz, 1H, NH), 8.44 (d, *J* = 8 Hz, 1H, NH), 7.26-7.08 (m, 10H, Ar), 4.63 (m, 1H, αCH), 4.40 (m, 1H, αCH), 3.50 (m, 1H, αCH), 3.08 (dd, *J* = 4 and 12 Hz, 1H, βCH$_2$), 2.83 (dd, *J* = 8 and 12 Hz, 1H, βCH$_2$), 2.73 (dd, *J* = 4 and 12 Hz, 1H, βCH$_2$), 2.58 (m, *J* = 8 and 12 Hz, 1H, βCH$_2$), 2.05 (m, 1H, βCH), 0.88 (d, 3H, γCH$_3$), 0.80 (d, 3H, γCH$_3$). ^{13}C-NMR (100MHz, DMSO-*d*$_6$, TMS): δ (ppm) 173.6, 170.9, 169.6 (3 x CO); 138.4, 138.1, 129.9, 129.8, 128.7, 128.6, 126.9, 126.9 (Ar); 58.1, 54.5, 54.4, (3 x αC); 38.4, 37.8 (2 x βCH$_2$); 30.6 (βCH); 19.2, 17.6 (2 x γCH$_3$). MS (ESI): m/z 412.1 (M+H)$^+$, $C_{23}H_{29}N_3O_4$ requires 412.2.

^{1}H-NMR (400 MHz, DMSO-*d*$_6$, TMS)

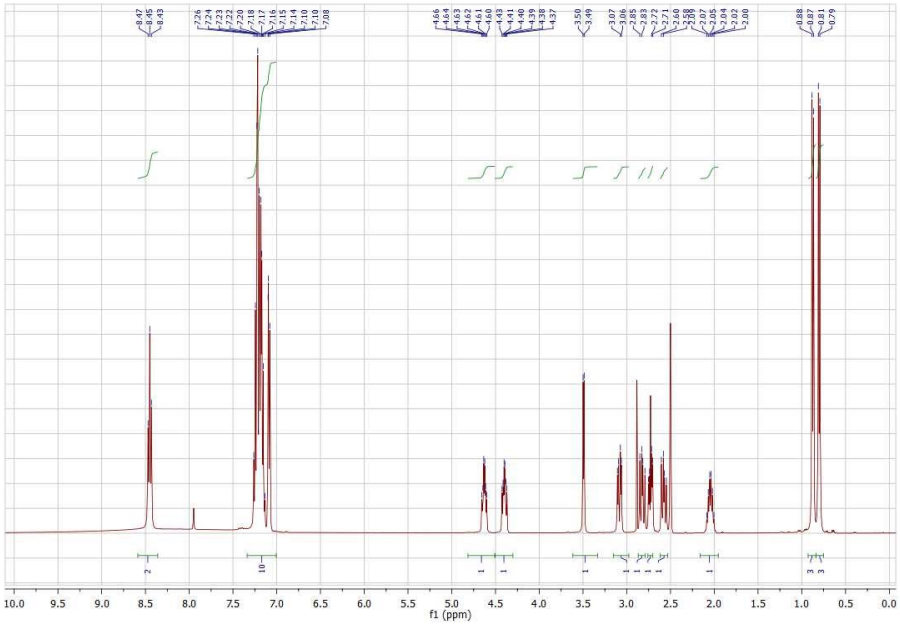

^{13}C-NMR (100MHz, DMSO-*d*$_6$, TMS)

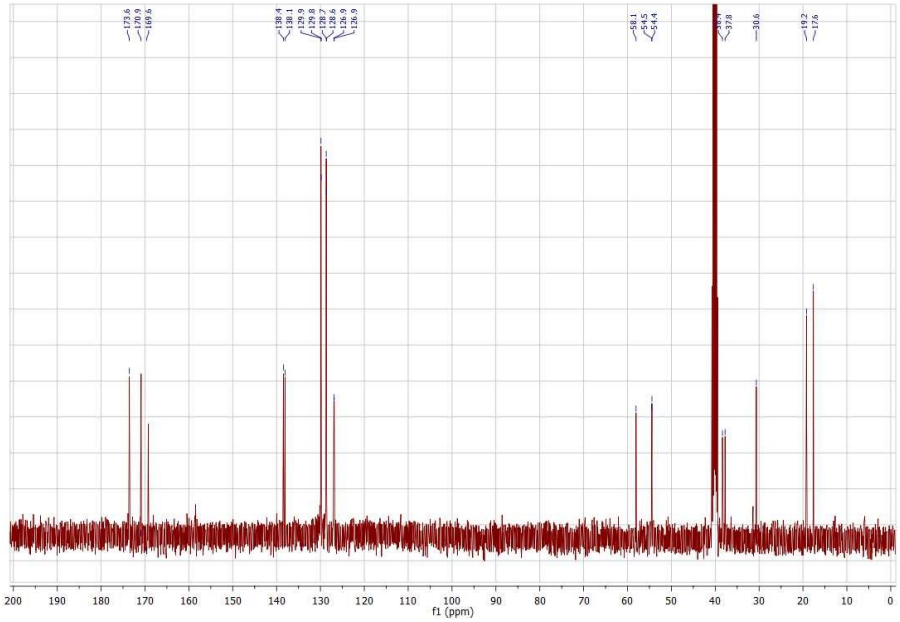

HPLC

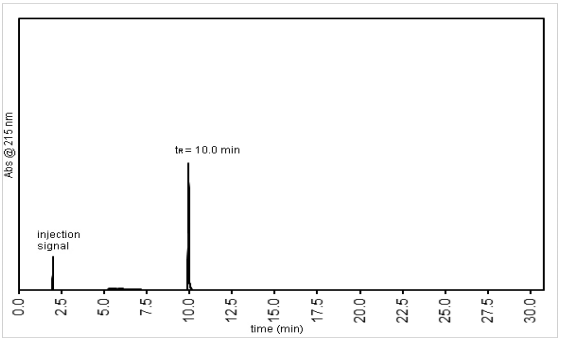

ESI-MS

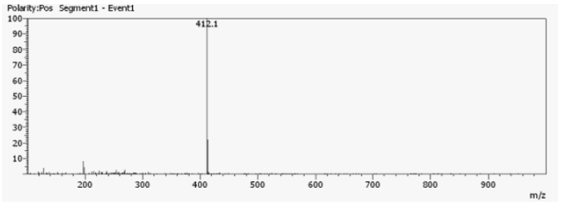

10. Spectroscopic data for vfF

^{1}H-NMR (400 MHz, DMSO-*d*$_6$, TMS): δ (ppm) 8.58 (d, *J* = 8 Hz, 1H, NH), 8.47 (d, *J* = 8 Hz, 1H, NH), 7.98 (s (br), 3H, NH_3^+), 7.24-7.09 (m, 10H, Ar), 4.64 (m, 1H, αCH), 4.43 (m, 1H, αCH), 3.59 (m, 1H, αCH), 3.07 (dd, *J* = 4 and 16 Hz,1H, βCH_2), 2.82 (dd, *J* = 8 and 16 Hz, 1H, βCH_2), 2.69 (dd, *J* = 4 and 16 Hz, 1H, βCH_2), 2.56 (m, *J* = 8 and 16 Hz, 1H, βCH_2), 2.08 (m, 1H, βCH), 0.91 (d, 3H, γCH_3), 0.85 (d, 3H, γCH_3). ^{13}C-NMR (100MHz, DMSO-*d*$_6$, TMS): δ (ppm) 173.3, 171.0, 168.1 (3 x CO), 138.0, 137.8, 130.4, 129.6, 129.6, 129.4, 128.6, 128.5, 126.9, 126.7 (Ar); 57.4, 54.3, 53.9, (3 x αC); 38.2, 37.4 (2 x βCH_2); 30.4 (βCH); 19.1, 17.9 (2 x γCH_3). MS (ESI): m/z 412.1 $(M+H)^+$, $C_{23}H_{29}N_3O_4$ requires 412.2.

^{1}H-NMR (400 MHz, DMSO-*d*$_6$, TMS)

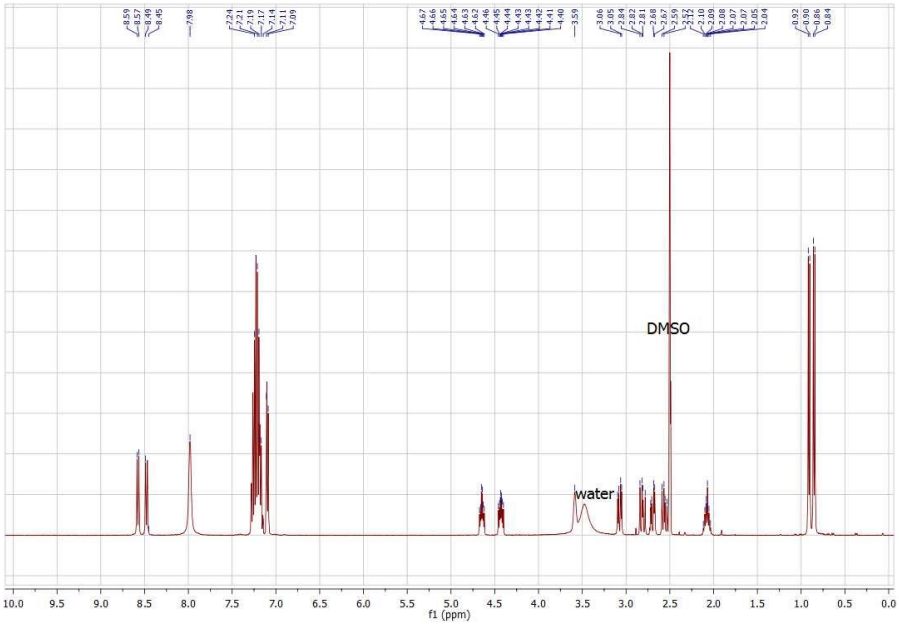

^{13}C-NMR (100MHz, DMSO-*d*$_6$, TMS)

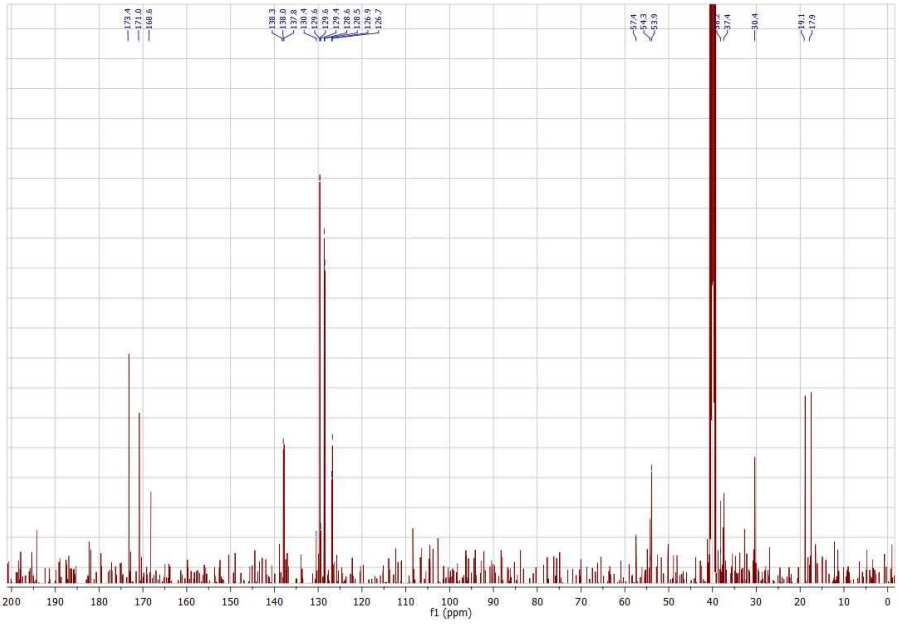

HPLC

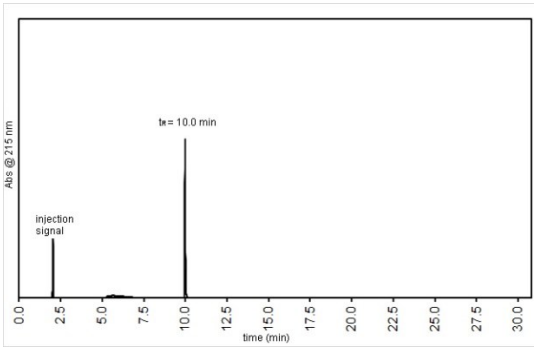

ESI-MS

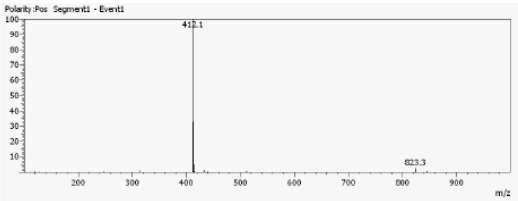

11. Spectroscopic data for Vff

^{1}H-NMR (400 MHz, DMSO-d_6, TMS): δ (ppm) 8.62 (d, J = 8 Hz, 2H, 2 x NH), 7.89 (s (br), 3H, NH_3^+), 7.32-7.15 (m, 10H, Ar), 4.75 (m, 1H, αCH), 4.45 (m, 1H, αCH), 3.53 (m, 1H, αCH), 3.10 (m, 2H, βCH_2), 2.93 (dd, J = 8 and 12 Hz, 1H, βCH_2), 2.64 (dd, J = 12 and 16 Hz, 1H, βCH_2), 1.78 (m, 1H, βCH), 0.63 (d, 3H, γCH_3), 0.36 (d, 3H, γCH_3). ^{13}C-NMR (100MHz, DMSO-d_6, TMS): δ (ppm) 173.4, 171.8, 168.6 (3 x CO); 138.0, 137.8, 129.6, 129.6, 128.7, 128.5, 127.0, 126.8 (Ar); 57.6, 54.2, 54.1, (3 x αC); 38.8, 37.4 (2 x βCH_2); 30.2 (βCH); 19.1, 16.7 (2 x γCH_3). MS (ESI): m/z 412.1 $(M+H)^+$, $C_{23}H_{29}N_3O_4$ requires 412.2.

^{1}H-NMR (400 MHz, DMSO-d_6, TMS)

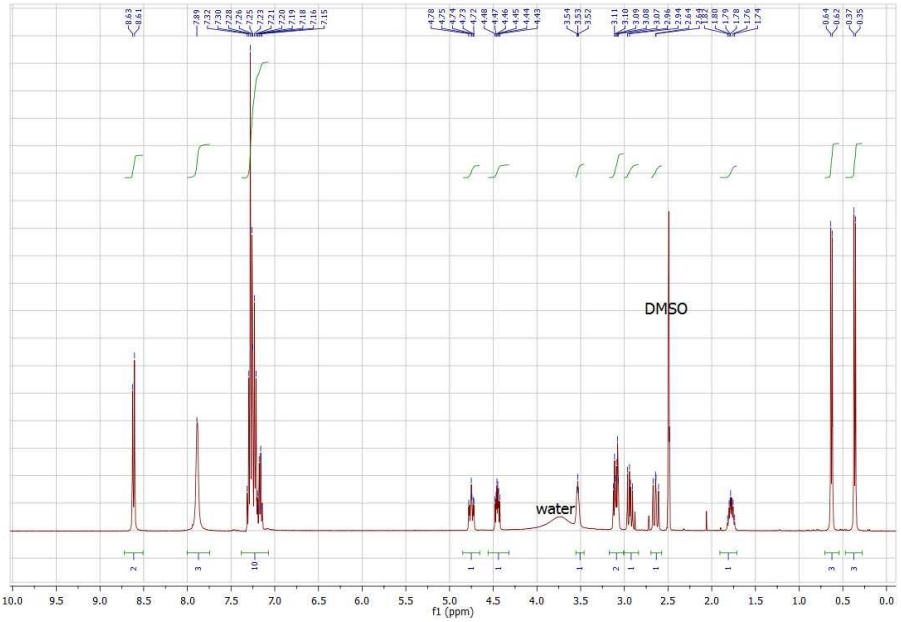

^{13}C-NMR (100MHz, DMSO-d_6, TMS)

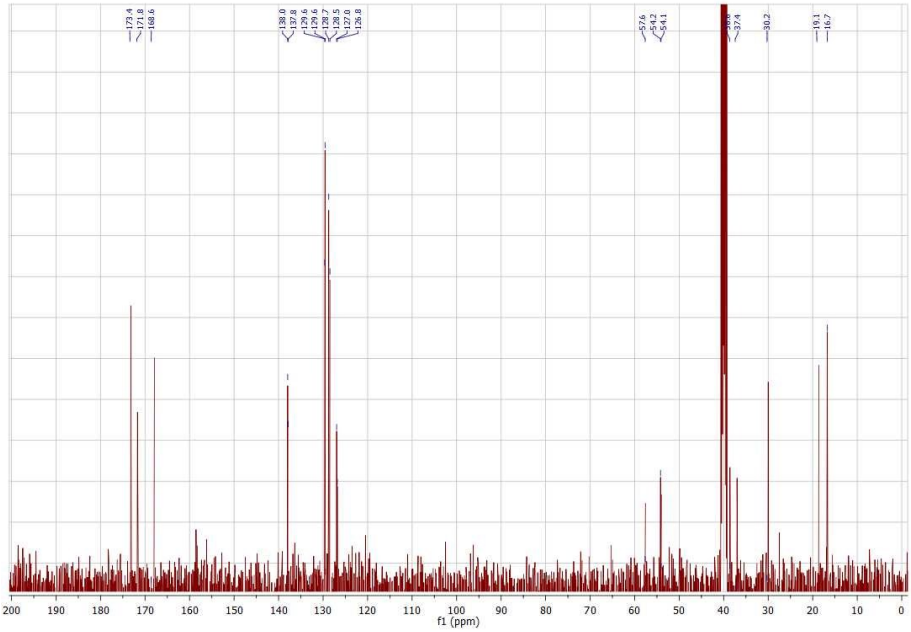

HPLC

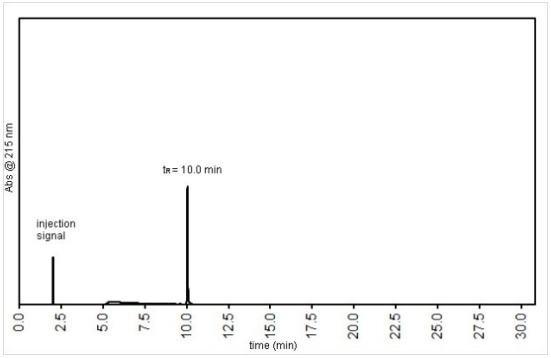

ESI-MS

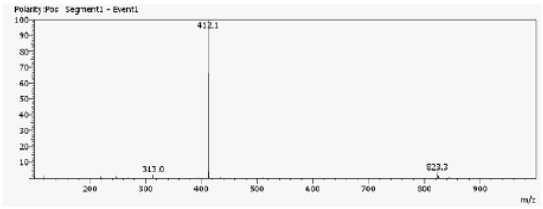

12. Spectroscopic data for vFf

^{1}H-NMR (400 MHz, DMSO-d_6, TMS): δ (ppm) 8.74 (d, J = 8 Hz, 1H, NH), 8.60 (d, J = 8 Hz, 1H, NH), 7.91 (s (br), 3H, NH_3^+), 7.30-7.11 (m, 10H, Ar), 4.80 (m, 1H, αCH), 4.53 (m, 1H, αCH), 3.55 (m, 1H, αCH), 3.14 (dd, J = 4 and 16 Hz, 1H, βCH_2), 2.85 (dd, J = 12 and 16 Hz, 1H, βCH_2), 2.67 (dd, J = 4 and 16 Hz, 1H, βCH_2), 2.38 (dd, J = 12 and 16 Hz, 1H, βCH_2), 1.80 (m, 1H, βCH), 0.66 (d, 3H, γCH_3), 0.40 (d, 3H, γCH_3). ^{13}C-NMR (100MHz, DMSO-d_6, TMS): δ (ppm) 173.3, 171.1, 167.9 (3 x CO); 137.8, 137.8, 129.7, 129.6, 128.6, 128.4, 127.0, 126.7 (Ar); 57.6, 54.0, 53.7, (3 x αC); 38.8, 37.6 (2 x βCH_2);

30.0 (βCH); 18.7, 16.7 (2 x γCH_3). MS (ESI): m/z 412.1 $(M+H)^+$, $C_{23}H_{29}N_3O_4$ requires 412.2.

^{1}H-NMR (400 MHz, DMSO-*d*$_6$, TMS)

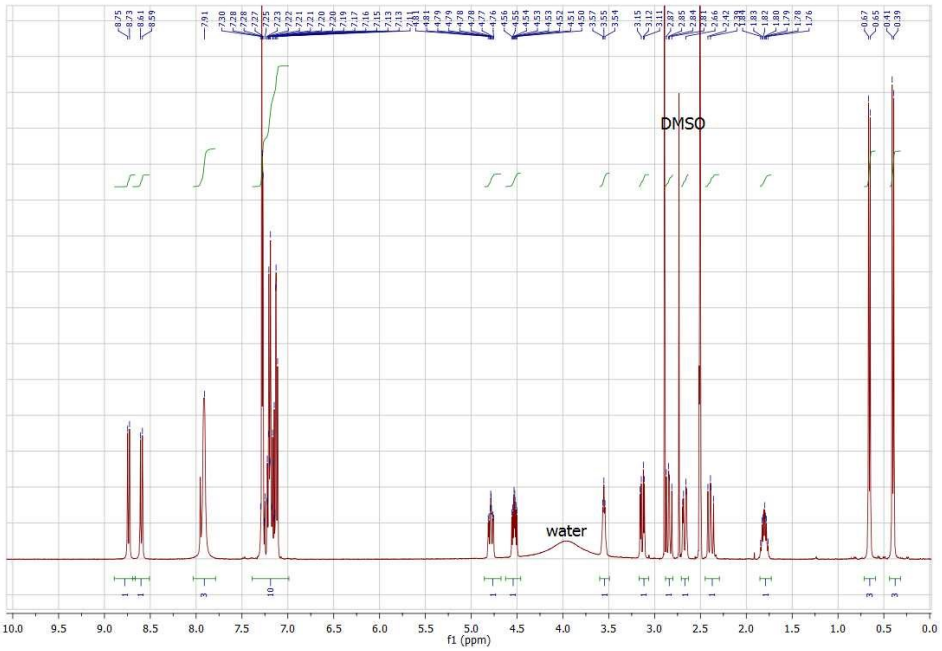

^{13}C-NMR (100MHz, DMSO-*d*$_6$, TMS)

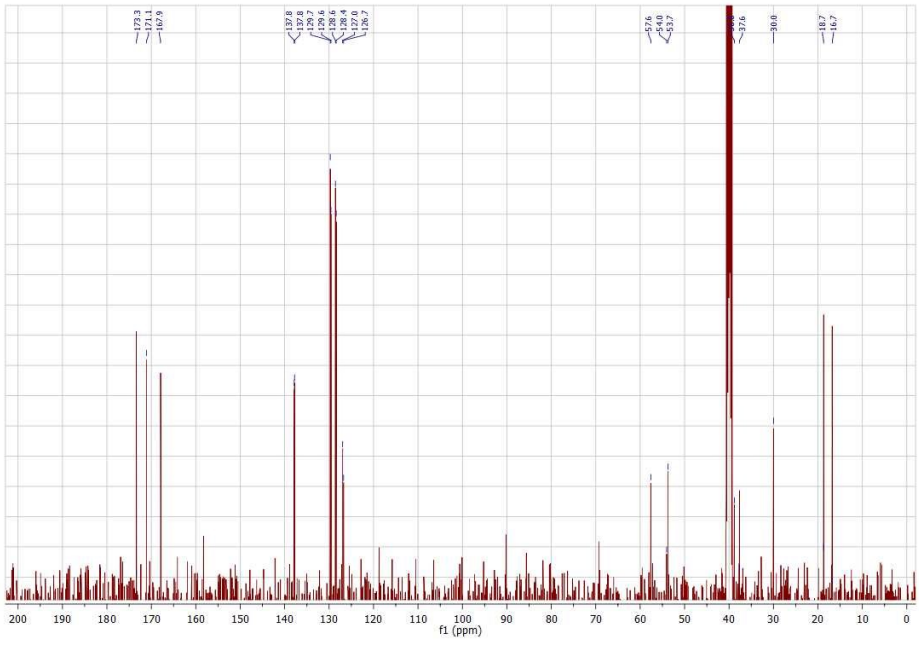

HPLC

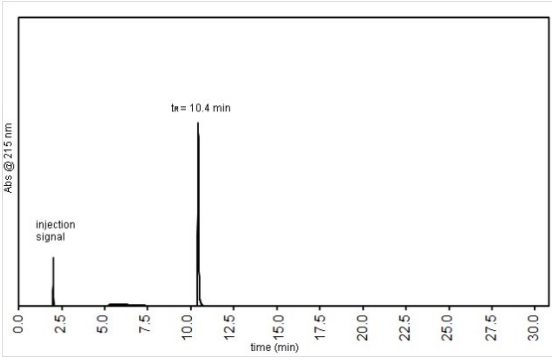

ESI-MS

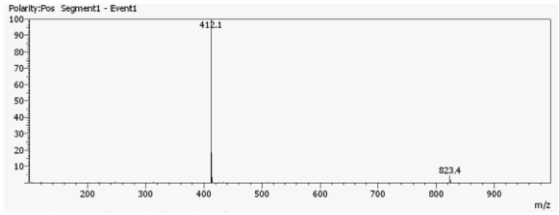

13. Spectroscopic data for vff

^{1}H-NMR (400 MHz, DMSO-*d*$_6$, TMS): δ (ppm) 8.57 (d, *J* = 8 Hz, 1H, NH), 8.50 (d, *J* = 8 Hz, 1H, NH), 8.03 (s (br), 3H, NH_3^+), 7.27-7.17 (m, 10H, Ar), 4.65-4.60 (m, 1H, αCH), 4.51-4.45 (m, 1H, αCH), 3.59 (m, 1H, αCH), 3.09 (dd, *J* = 4 and 16 Hz, 1H, βCH_2), 2.99 (dd, *J* = 4 and 16 Hz, 1H, βCH_2), 2.89 (dd, *J* = 8 and 16 Hz, 1H, βCH_2), 2.79 (dd, *J* = 8 and 16 Hz, 1H, βCH_2), 2.06 (m, 1H, βCH), 0.87 (d, 3H, γCH_3), 0.84 (d, 3H, γCH_3). ^{13}C-NMR (100MHz, DMSO-*d*$_6$, TMS): δ (ppm) 173.4, 170.9, 168.4 (3 x CO); 138.0, 129.8, 129.6, 128.8, 128.7, 127.0 (Ar); 57.6, 54.6, 53.9, (3 x αC); 38.2, 37.2 (2 x βCH_2); 30.5 (βCH); 19.0, 17.7 (2 x γCH_3). MS (ESI): m/z 412.1 $(M+H)^+$, $C_{23}H_{29}N_3O_4$ requires 412.2.

^{1}H-NMR (400 MHz, DMSO-*d*$_6$, TMS)

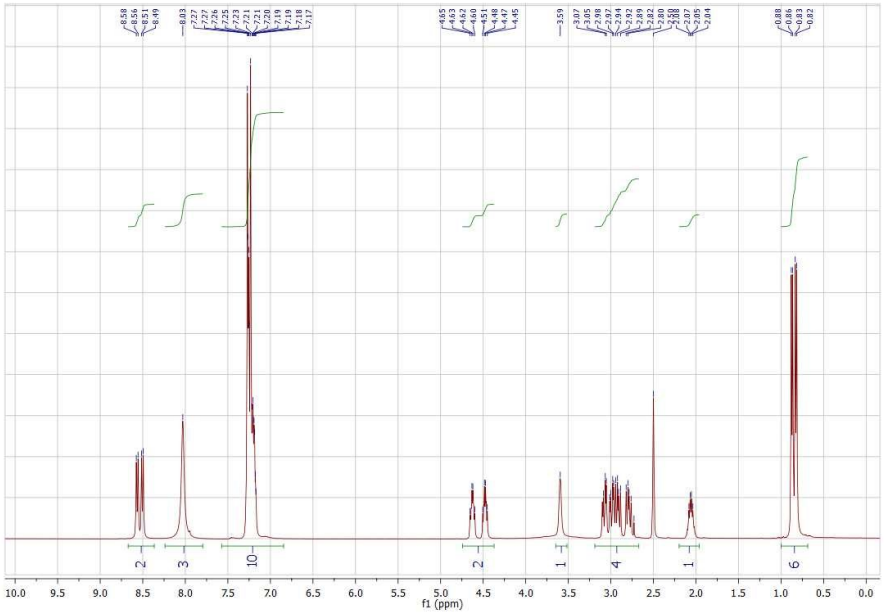

^{13}C-NMR (100MHz, DMSO-*d*$_6$, TMS)

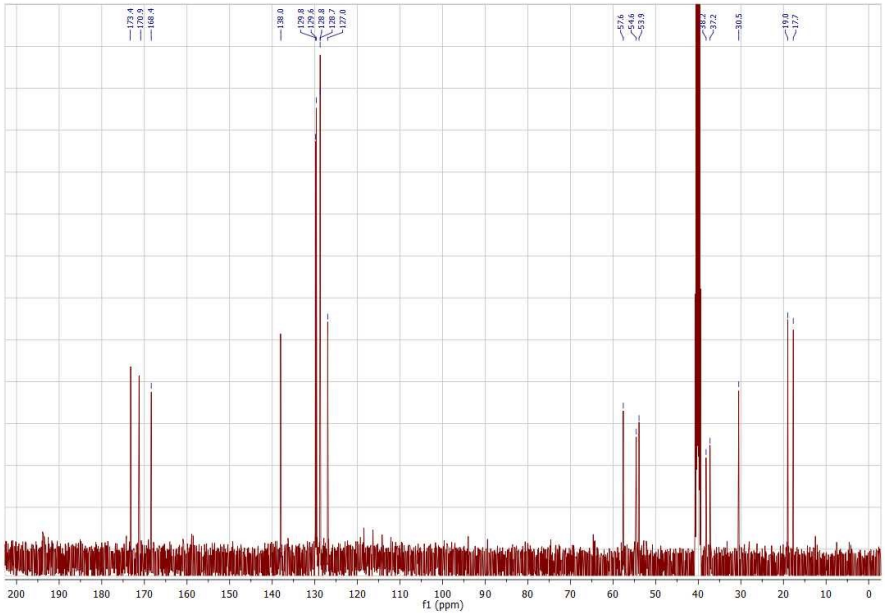

HPLC

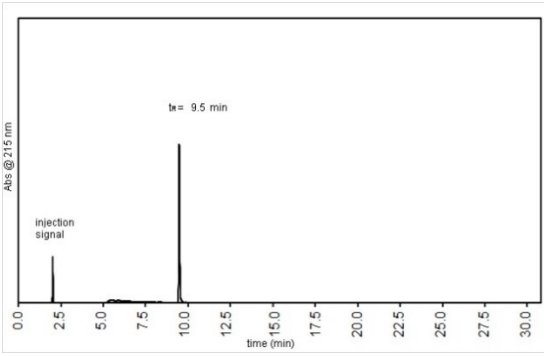

ESI-MS

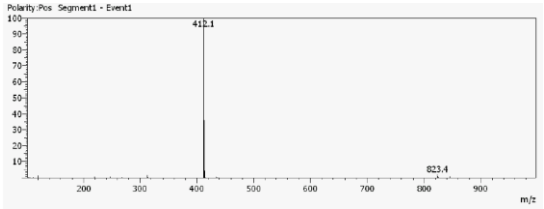

14. XRD spectra of Vff and vFf hydrogels

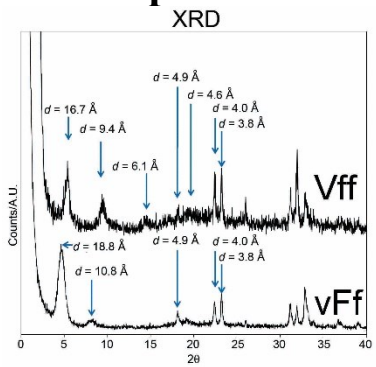

15. Molecular models

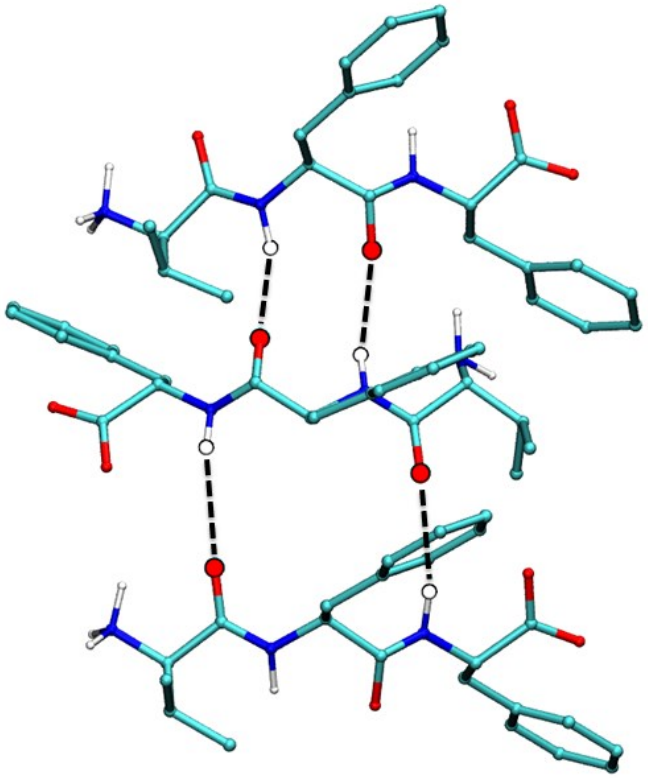

Figure SMAV1: Side view of a vFF trimer manually arranged as a antiparallel β-sheet. Atom pairs whose distance has been restrained (see Experimental section in the main text) are indicated by larger spheres and linked by dashed black arrows.

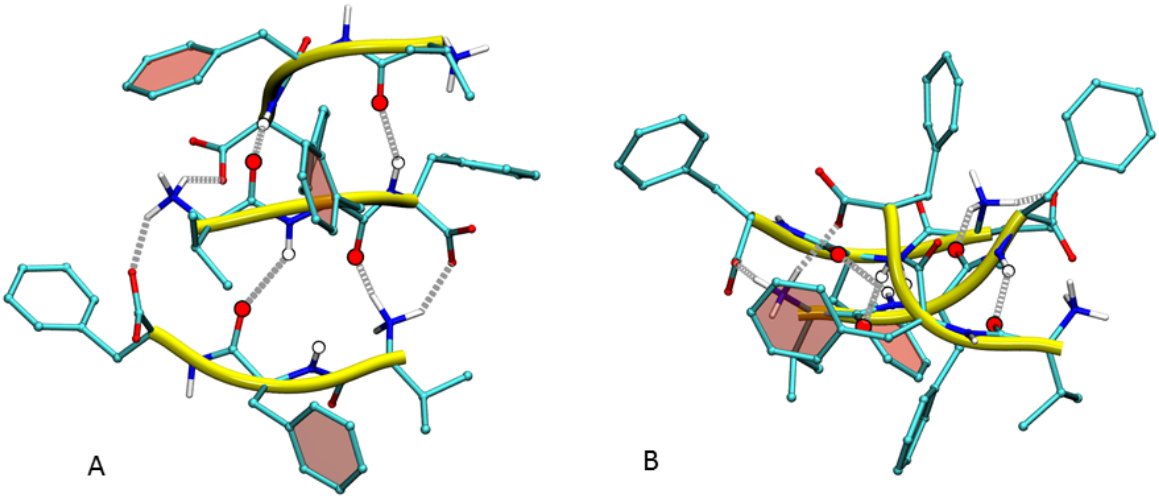

Figure SMAV2: Side (A) and top (B) views of a vFF trimer antiparallel β-sheet after structural optimization in explicit solvent. Amino acids are shown as CPK balls and sticks, and H-bonds between them are shown with dashed grey lines. The aromatic rings of central phenylalanines are also highlighted by transparent red planes. The backbone of each strand is also shown as a thick yellow tube.

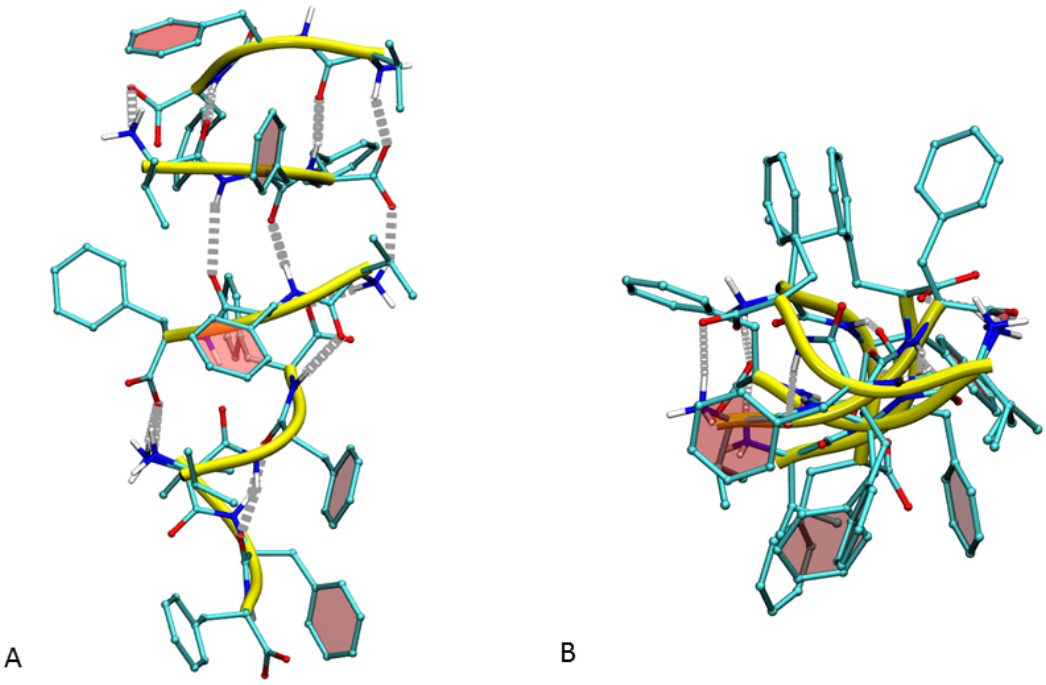

Figure SMAV3: Side (A) and top (B) views of a vFF pentamer antiparallel β-sheet after structural optimization in explicit solvent. Amino acids are shown as CPK balls and sticks, and H-bonds between them are shown with dashed grey lines. The aromatic rings of central phenylalanines are also highlighted by transparent red planes. The backbone of each strand is also shown as a thick yellow tube.

16. Brightfield microscopy images of fibroblast cells inside peptide gels at 24h

vFF peptide gel, focusing just below the gel surface

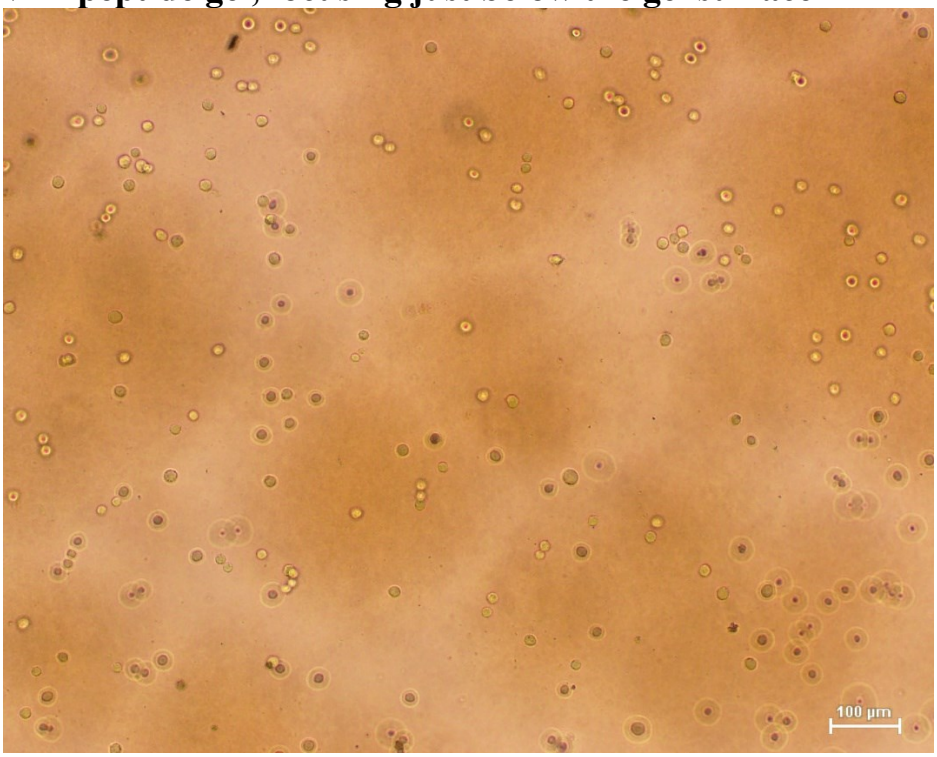

vFF peptide gel, focusing deep in the gel, just above the well bottom

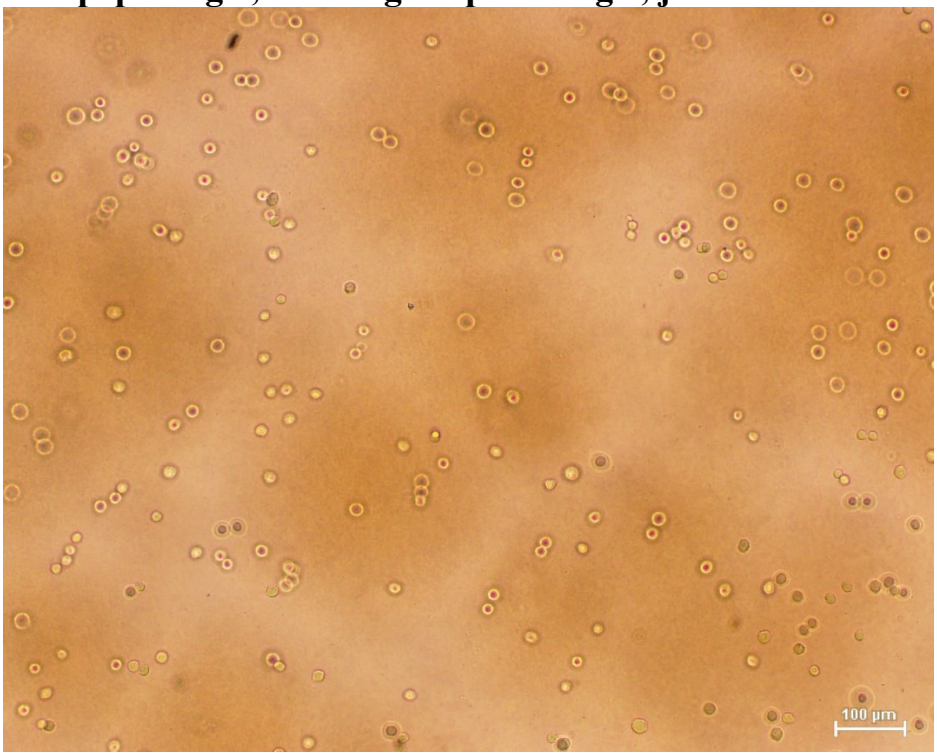

Vff peptide gel, focusing just below the gel surface

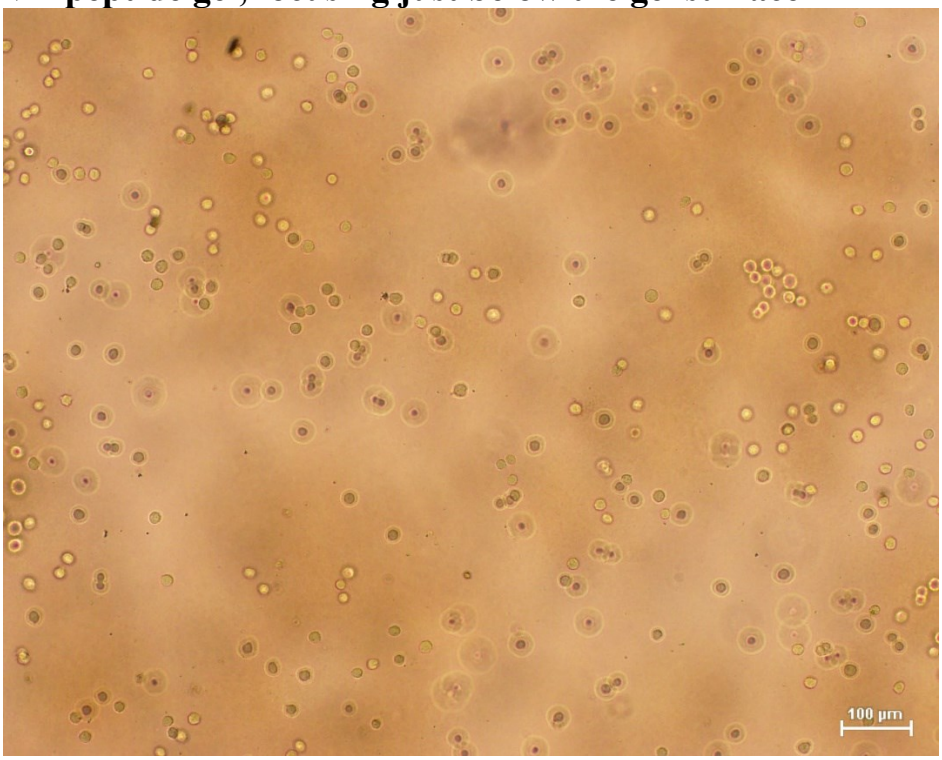

Vff peptide gel, focusing deep in the gel, just above the well bottom

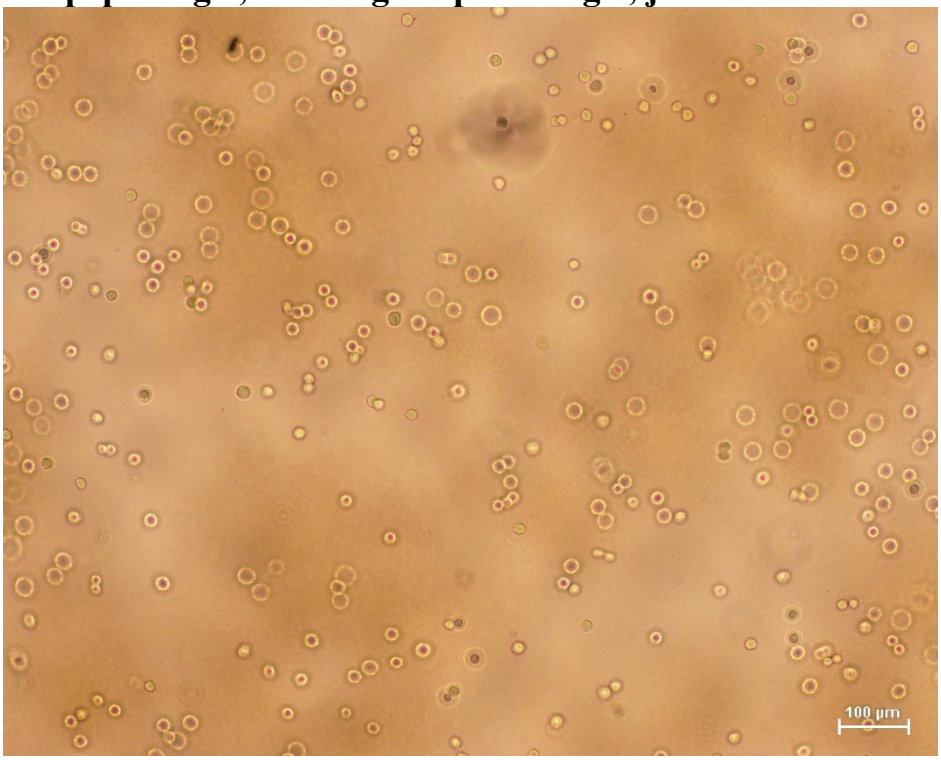

17. Protease degradation tests for gelling peptides in sol and in gel

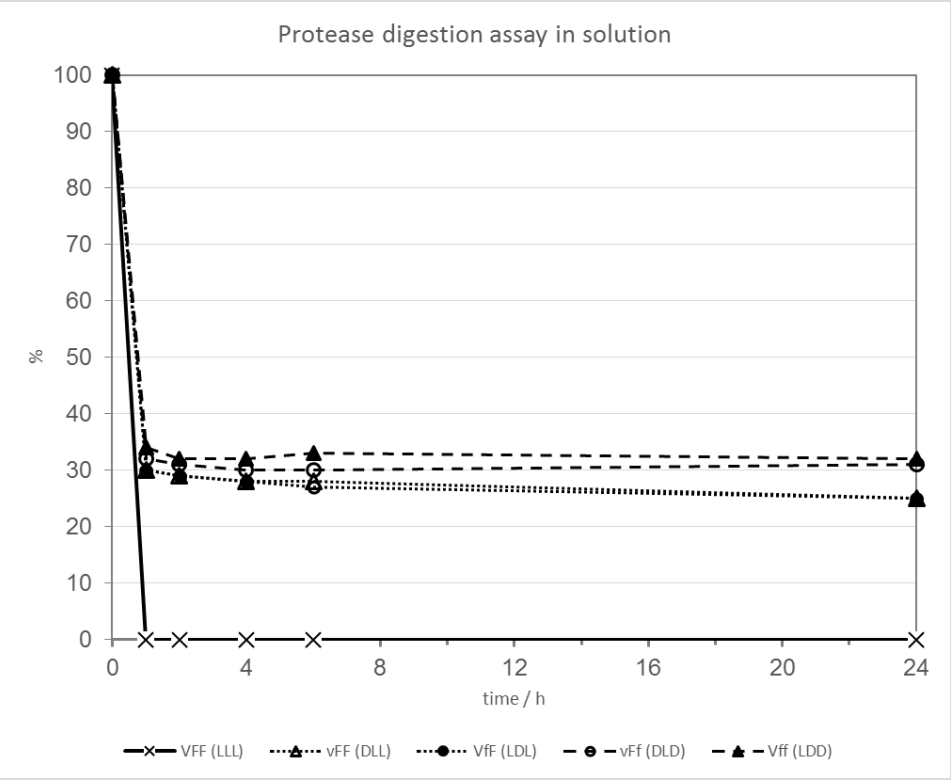

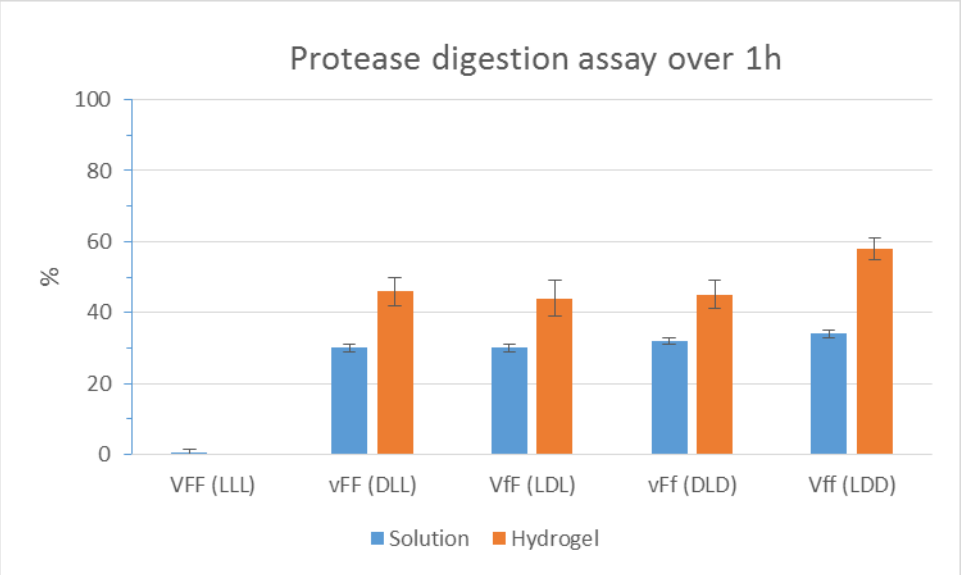

Note: By visual observation of the gels, ca. 70% for vFF and Vff, and ca. 50% for VfF and vFf, by eye, remained after the protease assay. This is substantially higher than calculated by HPLC (see orange bars in graph above). We suggest the HPLC data is an under-estimate owing to the fact that as soon as the gels were disassembled and peptides were dissolved, in preparation for HPLC, further hydrolysis rapidly occurred by the residual active protease on active-site now-exposed tripeptide(s).